



Quasi-physical modeling of robot IRB 120 using Simscape Multibody for dynamic and control simulation

Le Ngoc TRUC^{1,2}, Nguyen Tung LAM^{3,*}

¹Institute for Control Engineering and Automation, Hanoi University of Science and Technology, Hanoi, Vietnam

²Faculty of Automobile Engineering, Hung Yen University of Technology and Education, Hung Yen, Vietnam

³Department of Industrial Automation, School of Electrical Engineering,
Hanoi University of Science and Technology, Hanoi, Vietnam

Received: 24.09.2019

Accepted/Published Online: 08.01.2020

Final Version: 29.07.2020

Abstract: The mathematical model of robot that is used to design control algorithms is mostly reused in numerical simulations as a virtual plant. The use of same model for both control design and simulation tasks makes the outcome idealized. Consequently, the effectiveness and feasibility of designed control methodologies when applied in practice seem to be questionable. The paper presents the quasi-physical modeling of a 6-DOF robot using MATLAB/Simscape Multibody for dynamic and control simulation. The bodies of the robot are assembled into a physical network with connections that represent physical domains. The dynamical manners of the quasi-physical model are close to that of real robot manipulators. This model can be exploited to verify the accuracy of mathematical models. After designing process, the control laws are validated with this model instead of an ideal mathematical model or an actual expensive prototype. The efficiency of the proposed modeling approach is demonstrated through the dynamic and control simulation of robot IRB 120.

Key words: Dynamic model, quasi-physical modeling, robot manipulator, Simscape Multibody

1. Introduction

For robot dynamics modeling, many well-known techniques based on the Euler-Lagrange equations are published [1–6]. Control algorithms are mostly designed based on mathematical models. The use of the same mathematical model, in control design as an object and in simulation as a plant, idealizes the system. Hence, the control performance is far away from reality. Additionally, it is not easy to add original friction, actuator dynamics, and other nonlinearities to mathematical models. These drawbacks can be overcome in quasi-physical models generated and simulated by Simscape Multibody. This is an effective approach for representing multibody systems because of its compliance with real physical plants. Based on this model, the system responses can be evaluated assisting control adjustment. Simscape-based physical modeling has been used successfully in many different fields: PV generators in microgrid scenario [7], graphene based nano-electronic systems [8], power PIN diodes [9], wind turbine gearboxes [10], DC motors [11], 3-wheeled electric vehicles [12], and so on. For robot manipulators, several researches using this approach are presented, e.g., Furuta pendulums [13], hexapod robots [14], 3-RPS parallel robotics [15], 2-DOF robots [16], 5-DOF robotic manipulators [17], and successfully simulating a complicated mechanical system [18]. In [19], the paper deals with a system identification problem of Staubli RX-60 robot supported by least squares and particle swarm optimization methods through various measured data of the actual robot that are not always available in practice. In contrast, we look at proposing

*Correspondence: lam.nguyentung@hust.edu.vn

a quasi-model that can replace the actual robot in control designing phase. Our study deals with the quasi-physical model of robot IRB 120 reconstructed from its CAD model combined with Simscape Multibody for simulation and verification. The parameters of the Simscape model are obtained from a professional CAD software based robot part models. In this paper, firstly, the mathematical dynamic model of robot IRB 120 is built based on Euler-Lagrange equations (Section 2). Secondly, we build the quasi-physical model of the robot step-by-step from designing body geometry to completing the whole model (Section 3). Thirdly, the comparison between the behaviors of the mathematical model and the quasi-physical model in term of dynamic and control simulation is given (Section 4). Finally, some important conclusions are discussed in Section 5.

2. Mathematical dynamic modeling

2.1. Dynamic modeling based on Euler-Lagrange equations, briefly

The general dynamic model of a n -link robot manipulator is as follows (without considering friction):

$$\boldsymbol{\tau} = \mathbf{M}\ddot{\mathbf{q}} + \mathbf{C}\dot{\mathbf{q}} + \mathbf{g}, \quad (1)$$

where $\boldsymbol{\tau} \in \mathbb{R}^n$ is the applied force/torque vector; $\mathbf{q} \in \mathbb{R}^n$ is the vector of joint variables; $\mathbf{M} \in \mathbb{R}^{n \times n}$ is the generalized inertia matrix; $\mathbf{C} \in \mathbb{R}^{n \times n}$ is the Coriolis/centrifugal matrix; and $\mathbf{g} \in \mathbb{R}^n$ is the gravity vector term. The generalized inertia matrix [20–25] and the vectors of Coriolis/centrifugal, gravity terms [26, 27] are given by

$$\mathbf{M} = \sum_{i=1}^n \left(m_i (\mathbf{J}_{T_i}^0)^T \mathbf{J}_{T_i}^0 + \mathbf{J}_{R_i}^T \mathbf{I}_i \mathbf{J}_{R_i} \right) \quad (2)$$

$$\mathbf{C} = \frac{1}{2} \left[\frac{\partial \mathbf{M}}{\partial \mathbf{q}} (\mathbf{1}_n \otimes \dot{\mathbf{q}}) + \frac{\partial \mathbf{M}}{\partial \dot{\mathbf{q}}} (\dot{\mathbf{q}} \otimes \mathbf{1}_n) - \left(\frac{\partial \mathbf{M}}{\partial \dot{\mathbf{q}}} (\dot{\mathbf{q}} \otimes \mathbf{1}_n) \right)^T \right], \quad \mathbf{g} = \left(\frac{\partial P}{\partial \mathbf{q}} \right)^T \quad (3)$$

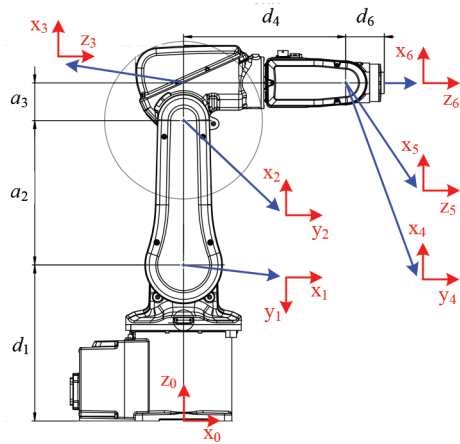
where m_i is the mass of link i ; $\mathbf{I}_i \in \mathbb{R}^{3 \times 3}$ is the link inertia tensor with respect to the frame attached at the link centroid and parallel to the corresponding attached frame; $\mathbf{1}_n \in \mathbb{R}^{n \times n}$ is the identity matrix; \otimes denotes Kronecker product operator defined in [28–30]; P is the total potential energy, \mathbf{J}_{R_i} , and $\mathbf{J}_{T_i}^0 \in \mathbb{R}^{3 \times n}$ are the rotational and translational Jacobian matrices calculated as

$$P = - \sum_{i=1}^n m_i (\mathbf{g}^0)^T \mathbf{p}_{C_i}^0, \quad \mathbf{J}_{R_i} = \frac{\partial \boldsymbol{\omega}_i}{\partial \dot{\mathbf{q}}}, \quad \mathbf{J}_{T_i}^0 = \frac{\partial \mathbf{v}_i^0}{\partial \dot{\mathbf{q}}} = \frac{\partial \mathbf{p}_{C_i}^0}{\partial \dot{\mathbf{q}}} \quad (4)$$

where every vector variable expressed in the base frame is denoted by superscript “0”, and in the corresponding attached frame has no superscript; $\mathbf{g}^0 = [0, 0, -g]^T$ is the gravitational acceleration vector, $g = 9.807 \text{ m/s}^2$; $\boldsymbol{\omega}_i \in \mathbb{R}^3$ is the link angular velocity; $\mathbf{v}_i^0 \in \mathbb{R}^3$ is the link linear velocity; and $\mathbf{p}_{C_i}^0 \in \mathbb{R}^3$ is the position of link centroid.

2.2. Mathematical dynamic modeling of robot IRB 120

Robot IRB 120, which is one type of 6-DOF industrial robots produced by ABB corporation, has 6 revolute joints. The robot configuration with attached frames and the D-H parameters are described in Figure 1. The homogeneous transformation matrices between 2 consecutive frames, \mathbf{T}_i^{i-1} , are derived from Figure 1 as



(a) The attached frames

Joint i	θ_i [rad]	d_i [m]	a_i [m]	α_i [rad]
1	q_1	$d_1 = 0.290$	$a_1 = 0$	$\alpha_1 = -\pi/2$
2	$q_2 - \pi/2$	$d_2 = 0$	$a_2 = 0.27$	$\alpha_2 = 0$
3	q_3	$d_3 = 0$	$a_3 = 0.07$	$\alpha_3 = -\pi/2$
4	q_4	$d_4 = 0.302$	$a_4 = 0$	$\alpha_4 = \pi/2$
5	q_5	$d_5 = 0$	$a_5 = 0$	$\alpha_5 = -\pi/2$
6	q_6	$d_6 = 0.072$	$a_6 = 0$	$\alpha_6 = 0$

(b) D-H parameters

Figure 1. The attached frames and D-H parameters of robot IRB 120.

$$\begin{aligned}
 \mathbf{T}_1^0 &= \begin{bmatrix} c_1 & 0 & -s_1 & 0 \\ s_1 & 0 & c_1 & 0 \\ 0 & -1 & 0 & d_1 \\ 0 & 0 & 0 & 1 \end{bmatrix} & \mathbf{T}_2^1 &= \begin{bmatrix} s_2 & c_2 & 0 & a_2 s_2 \\ -c_2 & s_2 & 0 & -a_2 c_2 \\ 0 & 0 & 1 & 0 \\ 0 & 0 & 0 & 1 \end{bmatrix} & \mathbf{T}_3^2 &= \begin{bmatrix} c_3 & 0 & -s_3 & a_3 c_3 \\ s_3 & 0 & c_3 & a_3 s_3 \\ 0 & -1 & 0 & 0 \\ 0 & 0 & 0 & 1 \end{bmatrix} \\
 \mathbf{T}_4^3 &= \begin{bmatrix} c_4 & 0 & s_4 & 0 \\ s_4 & 0 & -c_4 & 0 \\ 0 & 1 & 0 & d_4 \\ 0 & 0 & 0 & 1 \end{bmatrix} & \mathbf{T}_5^4 &= \begin{bmatrix} c_5 & 0 & -s_5 & 0 \\ s_5 & 0 & c_5 & 0 \\ 0 & -1 & 0 & 0 \\ 0 & 0 & 0 & 1 \end{bmatrix} & \mathbf{T}_6^5 &= \begin{bmatrix} c_6 & -s_6 & 0 & 0 \\ s_6 & c_6 & 0 & 0 \\ 0 & 0 & 1 & d_6 \\ 0 & 0 & 0 & 1 \end{bmatrix} \tag{5}
 \end{aligned}$$

where s_i , c_i , s_{ij} , and c_{ij} represent $\sin(q_i)$, $\cos(q_i)$, $\sin(q_i + q_j)$, and $\cos(q_i + q_j)$, respectively, ($i, j = 1, \dots, 6$). From (5), 6 homogeneous transformation matrices $\mathbf{T}_1^0, \dots, \mathbf{T}_6^0$ can be developed. In order to demonstrate the results and due to space limitation, only matrix \mathbf{T}_6^0 is displayed as follows:

$$\begin{aligned}
 T_6^0(1, 1) &= c_1 (c_4 c_5 c_6 - s_4 s_6) s_{23} + s_5 c_{23} c_1 c_6 + s_1 (c_5 c_6 s_4 + c_4 s_6) \\
 T_6^0(2, 1) &= s_1 (c_4 c_5 c_6 - s_4 s_6) s_{23} + s_1 s_5 c_{23} c_6 - c_1 (c_5 c_6 s_4 + c_4 s_6) \\
 T_6^0(3, 1) &= c_4 c_5 c_6 c_{23} - c_6 s_5 s_{23} - c_{23} s_4 s_6 \\
 T_6^0(1, 2) &= -c_1 (c_4 c_5 s_6 + c_6 s_4) s_{23} - s_5 c_{23} c_1 s_6 - s_1 (c_5 s_4 s_6 - c_4 c_6) \\
 T_6^0(2, 2) &= -s_1 (c_4 c_5 s_6 + c_6 s_4) s_{23} - s_1 s_5 c_{23} s_6 + c_1 (c_5 s_4 s_6 - c_4 c_6) \\
 T_6^0(3, 2) &= -c_4 c_5 c_{23} s_6 - c_6 c_{23} s_4 + s_5 s_6 s_{23} \\
 T_6^0(1, 3) &= -c_1 c_4 s_5 s_{23} + c_1 c_5 c_{23} - s_1 s_4 s_5 \\
 T_6^0(2, 3) &= -c_4 s_1 s_5 s_{23} + c_1 s_4 s_5 + c_5 c_{23} s_1 \\
 T_6^0(3, 3) &= -c_4 c_{23} s_5 - c_5 s_{23}
 \end{aligned}$$

$$\begin{aligned}
 T_6^0(1, 4) &= c_1 (c_5 d_6 + d_4) c_{23} - c_1 (c_4 d_6 s_5 - a_3) s_{23} - s_1 s_4 s_5 d_6 + c_1 a_2 s_2 \\
 T_6^0(2, 4) &= s_1 (c_5 d_6 + d_4) c_{23} - s_1 (c_4 d_6 s_5 - a_3) s_{23} + s_4 s_5 c_1 d_6 + s_1 a_2 s_2 \\
 T_6^0(3, 4) &= (-c_4 d_6 s_5 + a_3) c_{23} - (c_5 d_6 + d_4) s_{23} + a_2 c_2 + d_1
 \end{aligned} \tag{6}$$

The rotational Jacobian matrices are obtained as

$$\begin{aligned}
 \mathbf{J}_{R_1} &= \frac{\partial \boldsymbol{\omega}_1}{\partial \dot{\mathbf{q}}} = \begin{bmatrix} 0 & 0 & 0 & 0 & 0 & 0 \\ -1 & 0 & 0 & 0 & 0 & 0 \\ 0 & 0 & 0 & 0 & 0 & 0 \end{bmatrix}, & \mathbf{J}_{R_2} &= \frac{\partial \boldsymbol{\omega}_2}{\partial \dot{\mathbf{q}}} = \begin{bmatrix} c_2 & 0 & 0 & 0 & 0 & 0 \\ -s_2 & 0 & 0 & 0 & 0 & 0 \\ 0 & 1 & 0 & 0 & 0 & 0 \end{bmatrix} \\
 \mathbf{J}_{R_3} &= \frac{\partial \boldsymbol{\omega}_3}{\partial \dot{\mathbf{q}}} = \begin{bmatrix} c_{23} & 0 & 0 & 0 & 0 & 0 \\ 0 & -1 & -1 & 0 & 0 & 0 \\ -s_{23} & 0 & 0 & 0 & 0 & 0 \end{bmatrix}, & \mathbf{J}_{R_4} &= \frac{\partial \boldsymbol{\omega}_4}{\partial \dot{\mathbf{q}}} = \begin{bmatrix} c_{23} c_4 & -s_4 & -s_4 & 0 & 0 & 0 \\ -s_{23} & 0 & 0 & 1 & 0 & 0 \\ c_{23} s_4 & c_4 & c_4 & 0 & 0 & 0 \end{bmatrix} \\
 \mathbf{J}_{R_5} &= \frac{\partial \boldsymbol{\omega}_5}{\partial \dot{\mathbf{q}}} = \begin{bmatrix} c_5 c_4 c_{23} - s_5 s_{23} & -c_5 s_4 & -c_5 s_4 & s_5 & 0 & 0 \\ -c_{23} s_4 & -c_4 & -c_4 & 0 & -1 & 0 \\ -s_5 c_4 c_{23} - c_5 s_{23} & s_5 s_4 & s_5 s_4 & c_5 & 0 & 0 \end{bmatrix}
 \end{aligned} \tag{7}$$

and \mathbf{J}_{R_6} with its elements represented as

$$\begin{aligned}
 J_{R_6}(1, 1) &= (c_6 c_4 c_5 - s_4 s_6) c_{23} - s_5 s_{23} c_6 & J_{R_6}(1, 4) &= s_5 c_6 \\
 J_{R_6}(2, 1) &= -(s_6 c_4 c_5 + c_6 s_4) c_{23} + s_5 s_{23} s_6 & J_{R_6}(2, 4) &= -s_5 s_6 \\
 J_{R_6}(3, 1) &= -s_5 c_4 c_{23} - c_5 s_{23} & J_{R_6}(3, 4) &= c_5 \\
 J_{R_6}(1, 2) &= -c_6 s_4 c_5 - s_6 c_4 & J_{R_6}(1, 5) &= -s_6 \\
 J_{R_6}(2, 2) &= s_4 s_6 c_5 - c_6 c_4 & J_{R_6}(2, 5) &= -c_6 \\
 J_{R_6}(3, 2) &= s_5 s_4 & J_{R_6}(3, 5) &= 0 \\
 J_{R_6}(1, 3) &= -c_6 s_4 c_5 - s_6 c_4 & J_{R_6}(1, 6) &= 0 \\
 J_{R_6}(2, 3) &= s_4 s_6 c_5 - c_6 c_4 & J_{R_6}(2, 6) &= 0 \\
 J_{R_6}(3, 3) &= s_5 s_4 & J_{R_6}(3, 6) &= 1
 \end{aligned} \tag{8}$$

Let us denote the link centroid with respect to the corresponding attached frame by $\mathbf{r}_{C_i} = [x_{C_i}, y_{C_i}, z_{C_i}]^T$. The link centroid with respect to the base frame is computed from \mathbf{r}_{C_i} by $[(\mathbf{p}_{C_i}^0)^T, 1]^T = \mathbf{T}_i^0 [\mathbf{r}_{C_i}^T, 1]^T$ as

$$\begin{aligned}
 \mathbf{p}_{C_1}^0 &= \begin{bmatrix} c_1 x_{C_1} - s_1 z_{C_1} \\ c_1 z_{C_1} + s_1 x_{C_1} \\ -y_{C_1} + d_1 \end{bmatrix}, & \mathbf{p}_{C_2}^0 &= \begin{bmatrix} ((a_2 + x_{C_2}) s_2 + y_{C_2} c_2) c_1 - s_1 z_{C_2} \\ ((a_2 + x_{C_2}) s_2 + y_{C_2} c_2) s_1 + c_1 z_{C_2} \\ -s_2 y_{C_2} + (a_2 + x_{C_2}) c_2 + d_1 \end{bmatrix} \\
 \mathbf{p}_{C_3}^0 &= \begin{bmatrix} c_1 (a_3 + x_{C_3}) s_{23} + a_2 c_1 s_2 + c_1 c_{23} z_{C_3} + s_1 y_{C_3} \\ s_1 (a_3 + x_{C_3}) s_{23} + a_2 s_1 s_2 + s_1 c_{23} z_{C_3} - c_1 y_{C_3} \\ (a_3 + x_{C_3}) c_{23} + a_2 c_2 - s_{23} z_{C_3} + d_1 \end{bmatrix}
 \end{aligned} \tag{9}$$

and vectors $\mathbf{p}_{C_4}^0, \mathbf{p}_{C_5}^0, \mathbf{p}_{C_6}^0$ with their elements are as follows:

$$\begin{aligned}
 p_{C_4}^0(1,1) &= c_1 (c_4x_{C_4} + s_4z_{C_4} + a_3) s_{23} + c_1 (d_4 + y_{C_4}) c_{23} + c_1 a_2 s_2 - s_1 (c_4z_{C_4} - s_4x_{C_4}) \\
 p_{C_4}^0(2,1) &= s_1 (c_4x_{C_4} + s_4z_{C_4} + a_3) s_{23} + s_1 (d_4 + y_{C_4}) c_{23} + s_1 a_2 s_2 + c_1 (c_4z_{C_4} - s_4x_{C_4}) \\
 p_{C_4}^0(3,1) &= (c_4x_{C_4} + s_4z_{C_4} + a_3) c_{23} - (d_4 + y_{C_4}) s_{23} + a_2 c_2 + d_1
 \end{aligned} \tag{10}$$

$$\begin{aligned}
 p_{C_5}^0(1,1) &= ((c_5x_{C_5} - s_5z_{C_5}) c_4 - s_4y_{C_5} + a_3) c_1 s_{23} + c_1 (c_5z_{C_5} + s_5x_{C_5} + d_4) c_{23} + c_1 a_2 s_2 \\
 &\quad + (c_4y_{C_5} + s_4 (c_5x_{C_5} - s_5z_{C_5})) s_1 \\
 p_{C_5}^0(2,1) &= s_1 ((c_5x_{C_5} - s_5z_{C_5}) c_4 - s_4y_{C_5} + a_3) s_{23} + s_1 (c_5z_{C_5} + s_5x_{C_5} + d_4) c_{23} + s_1 a_2 s_2 \\
 &\quad - (c_4y_{C_5} + s_4 (c_5x_{C_5} - s_5z_{C_5})) c_1
 \end{aligned}$$

$$p_{C_5}^0(3,1) = ((c_5x_{C_5} - s_5z_{C_5}) c_4 - s_4y_{C_5} + a_3) c_{23} - (c_5z_{C_5} + s_5x_{C_5} + d_4) s_{23} + a_2 c_2 + d_1 \tag{11}$$

$$\begin{aligned}
 p_{C_6}^0(1,1) &= c_1 (((c_6x_{C_6} - s_6y_{C_6}) c_5 - s_5 (d_6 + z_{C_6})) c_4 - (c_6y_{C_6} + s_6x_{C_6}) s_4 + a_3) s_{23} \\
 &\quad + ((d_6 + z_{C_6}) c_5 + (c_6x_{C_6} - s_6y_{C_6}) s_5 + d_4) c_1 c_{23} + c_1 a_2 s_2 \\
 &\quad + s_1 ((c_6y_{C_6} + s_6x_{C_6}) c_4 + s_4 ((c_6x_{C_6} - s_6y_{C_6}) c_5 - s_5 (d_6 + z_{C_6})))
 \end{aligned}$$

$$\begin{aligned}
 p_{C_6}^0(2,1) &= s_1 (((c_6x_{C_6} - s_6y_{C_6}) c_5 - s_5 (d_6 + z_{C_6})) c_4 - (c_6y_{C_6} + s_6x_{C_6}) s_4 + a_3) s_{23} \\
 &\quad + s_1 ((d_6 + z_{C_6}) c_5 + (c_6x_{C_6} - s_6y_{C_6}) s_5 + d_4) c_{23} + s_1 a_2 s_2 \\
 &\quad - ((c_6y_{C_6} + s_6x_{C_6}) c_4 + s_4 ((c_6x_{C_6} - s_6y_{C_6}) c_5 - s_5 (d_6 + z_{C_6}))) c_1
 \end{aligned}$$

$$\begin{aligned}
 p_{C_6}^0(3,1) &= (((c_6x_{C_6} - s_6y_{C_6}) c_5 - s_5 (d_6 + z_{C_6})) c_4 - c_6 s_4 y_{C_6} - s_4 s_6 x_{C_6} + a_3) c_{23} \\
 &\quad - ((d_6 + z_{C_6}) c_5 + (c_6x_{C_6} - s_6y_{C_6}) s_5 + d_4) s_{23} + a_2 c_2 + d_1
 \end{aligned} \tag{12}$$

Substituting (9)-(12) into (4) yields 6 translational Jacobian matrices $\mathbf{J}_{T_1}^0 \dots \mathbf{J}_{T_6}^0$; and for simplification, only $\mathbf{J}_{T_6}^0$ is presented to demonstrate the results:

$$\begin{aligned}
 J_{T_6}^0(1,1) &= -s_1 (((c_6x_{C_6} - s_6y_{C_6}) c_5 - s_5 (d_6 + z_{C_6})) c_4 - (c_6y_{C_6} + s_6x_{C_6}) s_4 + a_3) s_{23} \\
 &\quad - s_1 ((d_6 + z_{C_6}) c_5 + (c_6x_{C_6} - s_6y_{C_6}) s_5 + d_4) c_{23} - s_1 a_2 s_2 \\
 &\quad + ((c_6y_{C_6} + s_6x_{C_6}) c_4 + s_4 ((c_6x_{C_6} - s_6y_{C_6}) c_5 - s_5 (d_6 + z_{C_6}))) c_1
 \end{aligned}$$

$$\begin{aligned}
 J_{T_6}^0(2,1) &= c_1 (((c_6x_{C_6} - s_6y_{C_6}) c_5 - s_5 (d_6 + z_{C_6})) c_4 - (c_6y_{C_6} + s_6x_{C_6}) s_4 + a_3) s_{23} \\
 &\quad + ((d_6 + z_{C_6}) c_5 + (c_6x_{C_6} - s_6y_{C_6}) s_5 + d_4) c_1 c_{23} + c_1 a_2 s_2 \\
 &\quad + s_1 ((c_6y_{C_6} + s_6x_{C_6}) c_4 + s_4 ((c_6x_{C_6} - s_6y_{C_6}) c_5 - s_5 (d_6 + z_{C_6})))
 \end{aligned}$$

$$J_{T_6}^0(3,1) = 0$$

$$\begin{aligned}
 J_{T_6}^0(1,2) &= (((c_6x_{C_6} - s_6y_{C_6}) c_5 - s_5 (d_6 + z_{C_6})) c_4 - c_6 s_4 y_{C_6} - s_4 s_6 x_{C_6} + a_3) c_1 c_{23} \\
 &\quad - ((d_6 + z_{C_6}) c_5 + (c_6x_{C_6} - s_6y_{C_6}) s_5 + d_4) c_1 s_{23} + a_2 c_1 c_2
 \end{aligned}$$

$$\begin{aligned}
 J_{T_6}^0(2,2) &= (((c_6x_{C_6} - s_6y_{C_6}) c_5 - s_5 (d_6 + z_{C_6})) c_4 - c_6 s_4 y_{C_6} - s_4 s_6 x_{C_6} + a_3) s_1 c_{23} \\
 &\quad - ((d_6 + z_{C_6}) c_5 + (c_6x_{C_6} - s_6y_{C_6}) s_5 + d_4) s_1 s_{23} + a_2 s_1 c_2
 \end{aligned}$$

$$\begin{aligned}
J_{T_6}^0(3, 2) &= (((-c_6x_{C6} + s_6y_{C6})c_5 + s_5(d_6 + z_{C6}))c_4 + c_6s_4y_{C6} + s_4s_6x_{C6} - a_3)s_{23} \\
&\quad - ((d_6 + z_{C6})c_5 + (c_6x_{C6} - s_6y_{C6})s_5 + d_4)c_{23} - a_2s_2 \\
J_{T_6}^0(1, 3) &= (((c_6x_{C6} - s_6y_{C6})c_5 - s_5(d_6 + z_{C6}))c_4 - c_6s_4y_{C6} - s_4s_6x_{C6} + a_3)c_1c_{23} \\
&\quad - ((d_6 + z_{C6})c_5 + (c_6x_{C6} - s_6y_{C6})s_5 + d_4)c_1s_{23} \\
J_{T_6}^0(2, 3) &= (((c_6x_{C6} - s_6y_{C6})c_5 - s_5(d_6 + z_{C6}))c_4 - c_6s_4y_{C6} - s_4s_6x_{C6} + a_3)s_1c_{23} \\
&\quad - ((d_6 + z_{C6})c_5 + (c_6x_{C6} - s_6y_{C6})s_5 + d_4)s_1s_{23} \\
J_{T_6}^0(3, 3) &= (((-c_6x_{C6} + s_6y_{C6})c_5 + s_5(d_6 + z_{C6}))c_4 + c_6s_4y_{C6} + s_4s_6x_{C6} - a_3)s_{23} \\
&\quad - ((d_6 + z_{C6})c_5 + (c_6x_{C6} - s_6y_{C6})s_5 + d_4)c_{23} \\
J_{T_6}^0(1, 4) &= c_1((-c_6y_{C6} - s_6x_{C6})c_4 + ((-c_6x_{C6} + s_6y_{C6})c_5 + s_5(d_6 + z_{C6}))s_4)s_{23} \\
&\quad - (((-c_6x_{C6} + s_6y_{C6})c_5 + s_5(d_6 + z_{C6}))c_4 + (c_6y_{C6} + s_6x_{C6})s_4)s_1 \\
J_{T_6}^0(2, 4) &= s_1((-c_6y_{C6} - s_6x_{C6})c_4 + ((-c_6x_{C6} + s_6y_{C6})c_5 + s_5(d_6 + z_{C6}))s_4)s_{23} \\
&\quad + (((-c_6x_{C6} + s_6y_{C6})c_5 + s_5(d_6 + z_{C6}))c_4 + (c_6y_{C6} + s_6x_{C6})s_4)c_1 \\
J_{T_6}^0(3, 4) &= c_{23} (((-c_6x_{C6} + s_6y_{C6})c_5 + s_5(d_6 + z_{C6}))s_4 - (c_6y_{C6} + s_6x_{C6})c_4) \\
J_{T_6}^0(1, 5) &= -c_1((-c_6x_{C6} + s_6y_{C6})c_5 + s_5(d_6 + z_{C6}))c_{23} \\
&\quad - (c_1c_4s_{23} + s_1s_4)((d_6 + z_{C6})c_5 + (c_6x_{C6} - s_6y_{C6})s_5) \\
J_{T_6}^0(2, 5) &= -s_1((-c_6x_{C6} + s_6y_{C6})c_5 + s_5(d_6 + z_{C6}))c_{23} \\
&\quad + ((d_6 + z_{C6})c_5 + (c_6x_{C6} - s_6y_{C6})s_5)(-c_4s_1s_{23} + c_1s_4) \\
J_{T_6}^0(3, 5) &= -((d_6 + z_{C6})c_5 + (c_6x_{C6} - s_6y_{C6})s_5)c_4c_{23} \\
&\quad + s_{23}((-c_6x_{C6} + s_6y_{C6})c_5 + s_5(d_6 + z_{C6})) \\
J_{T_6}^0(1, 6) &= -c_1((c_4c_5y_{C6} + s_4x_{C6})c_6 + s_6(c_4c_5x_{C6} - s_4y_{C6}))s_{23} \\
&\quad - s_5c_1(c_6y_{C6} + s_6x_{C6})c_{23} - (c_5s_4y_{C6} - c_4x_{C6})s_1c_6 \\
&\quad - s_1s_6(c_5s_4x_{C6} + c_4y_{C6}) \\
J_{T_6}^0(2, 6) &= -s_1((c_4c_5y_{C6} + s_4x_{C6})c_6 + s_6(c_4c_5x_{C6} - s_4y_{C6}))s_{23} \\
&\quad - s_1s_5(c_6y_{C6} + s_6x_{C6})c_{23} + (c_5s_4y_{C6} - c_4x_{C6})c_1c_6 \\
&\quad + c_1s_6(c_5s_4x_{C6} + c_4y_{C6}) \\
J_{T_6}^0(3, 6) &= ((-c_4c_5y_{C6} - s_4x_{C6})c_6 + s_6(-c_4c_5x_{C6} + s_4y_{C6}))c_{23} \\
&\quad + (c_6y_{C6} + s_6x_{C6})s_5s_{23}
\end{aligned} \tag{13}$$

The generalized inertia matrix and the Coriolis/centrifugal matrix are obtained by applying the above necessary results to (2) and (3):

$$\mathbf{M} = \sum_{i=1}^6 \left(m_i (\mathbf{J}_{T_i}^0)^T \mathbf{J}_{T_i}^0 + \mathbf{J}_{R_i}^T \mathbf{I}_i \mathbf{J}_{R_i} \right) \quad (14)$$

$$\mathbf{C} = \frac{1}{2} \left[\frac{\partial \mathbf{M}}{\partial \mathbf{q}} (\mathbf{1}_6 \otimes \dot{\mathbf{q}}) + \frac{\partial \mathbf{M}}{\partial \dot{\mathbf{q}}} (\dot{\mathbf{q}} \otimes \mathbf{1}_6) - \left(\frac{\partial \mathbf{M}}{\partial \dot{\mathbf{q}}} (\dot{\mathbf{q}} \otimes \mathbf{1}_6) \right)^T \right] \quad (15)$$

The vector of gravity term is obtained via (3) with its 6 elements below:

$$g_1 = 0 \quad (16)$$

$$\begin{aligned} g_2 = & - \{ [(x_{C6}c_6m_6 - y_{C6}s_6m_6 + m_5x_{C5})c_5 - ((d_6 + z_{C6})m_6 + z_{C5}m_5)s_5]c_4 \\ & + x_{C4}m_4c_4 + (m_4z_{C4} - y_{C6}m_6c_6 - x_{C6}s_6m_6 - m_5y_{C5})s_4 \\ & + a_3m_6 + a_3m_5 + a_3m_4 + m_3(a_3 + x_{C3}) \} gs_{23} \\ & - \{ [(d_6 + z_{C6})m_6 + z_{C5}m_5]c_5 + s_5(x_{C6}c_6m_6 - y_{C6}s_6m_6 + m_5x_{C5}) \\ & + d_4m_6 + d_4m_5 + (d_4 + y_{C4})m_4 + z_{C3}m_3 \} gc_{23} \\ & - (a_2m_6 + a_2m_5 + a_2m_4 + (m_2 + m_3)a_2 + x_{C2}m_2)gs_2 - c_2m_2gy_{C2} \end{aligned}$$

$$\begin{aligned} g_3 = & - \{ [(x_{C6}c_6m_6 - y_{C6}s_6m_6 + m_5x_{C5})c_5 - ((d_6 + z_{C6})m_6 + z_{C5}m_5)s_5]c_4 \\ & + x_{C4}m_4c_4 + (m_4z_{C4} - c_6m_6y_{C6} - m_6s_6x_{C6} - m_5y_{C5})s_4 \\ & + a_3m_6 + a_3m_5 + a_3m_4 + m_3(a_3 + x_{C3}) \} gs_{23} \\ & - \{ [(d_6 + z_{C6})m_6 + z_{C5}m_5]c_5 + s_5(c_6m_6x_{C6} - y_{C6}s_6m_6 + m_5x_{C5}) \\ & + d_4m_6 + d_4m_5 + (d_4 + y_{C4})m_4 + z_{C3}m_3 \} gc_{23} \end{aligned}$$

$$\begin{aligned} g_4 = & - \{ (c_6m_6x_{C6} - y_{C6}s_6m_6 + m_5x_{C5})c_5 - ((d_6 + z_{C6})m_6 + z_{C5}m_5)s_5 + x_{C4}m_4 \} gc_{23}s_4 \\ & - (c_6m_6y_{C6} + m_6s_6x_{C6} - m_4z_{C4} + m_5y_{C5})gc_{23}c_4 \end{aligned}$$

$$\begin{aligned} g_5 = & - \{ [(d_6 + z_{C6})m_6 + z_{C5}m_5]c_5 + s_5(c_6m_6x_{C6} - y_{C6}s_6m_6 + m_5x_{C5}) \} gc_{23}c_4 \\ & - \{ (c_6m_6x_{C6} - y_{C6}s_6m_6 + m_5x_{C5})c_5 - ((d_6 + z_{C6})m_6 + z_{C5}m_5)s_5 \} gs_{23} \end{aligned}$$

$$g_6 = - \{ (c_4c_5y_{C6} + s_4x_{C6})c_6 + s_6(c_4c_5x_{C6} - s_4y_{C6}) \} m_6gc_{23} + (c_6y_{C6} + s_6x_{C6})m_6gs_{23}s_5 \quad (17)$$

3. Quasi-physical modeling of robot IRB 120 using Simscape Multibody

3.1. 3D CAD models of links

For a real robot manipulator, it is too difficult to get the precise information about the link centroids and inertia tensors of links. Hence, we exploit Autodesk Inventor which is a professional 3D mechanical design software to build the 3D CAD models of robot IRB 120 links for exploring those parameters (Figure 2). Based on the shape, structure, and material components of robot IRB 120 links, the approximated values of mass, link centroids, and inertia tensors can be achieved by performing the physics analysis method of Autodesk Inventor as follows:

Base: $m_0 = 8.659$

$$\begin{aligned}
 \text{Link 1: } m_1 = 4.248, \quad \mathbf{r}_{C_1} &= \begin{bmatrix} 0 \\ 0.054 \\ 0 \end{bmatrix}, \quad \mathbf{I}_1 = \begin{bmatrix} 19.699 & 0 & 0 \\ 0 & 14.484 & 0 \\ 0 & 0 & 19.952 \end{bmatrix} 10^{-3} \\
 \text{Link 2: } m_2 = 5.412, \quad \mathbf{r}_{C_2} &= \begin{bmatrix} -0.169 \\ 0 \\ 0 \end{bmatrix}, \quad \mathbf{I}_2 = \begin{bmatrix} 35.942 & 0 & 0 \\ 0 & 83.522 & 0 \\ 0 & 0 & 57.569 \end{bmatrix} 10^{-3} \\
 \text{Link 3: } m_3 = 4.077, \quad \mathbf{r}_{C_3} &= \begin{bmatrix} -0.012 \\ 0 \\ 0.023 \end{bmatrix}, \quad \mathbf{I}_3 = \begin{bmatrix} 17.562 & 0 & -1.993 \\ 0 & 23.140 & 0 \\ -1.993 & 0 & 11.589 \end{bmatrix} 10^{-3} \\
 \text{Link 4: } m_4 = 1.832, \quad \mathbf{r}_{C_4} &= \begin{bmatrix} 0 \\ -0.007 \\ 0 \end{bmatrix}, \quad \mathbf{I}_4 = \begin{bmatrix} 7.247 & 0 & 0 \\ 0 & 3.919 & 0 \\ 0 & 0 & 5.551 \end{bmatrix} 10^{-3} \\
 \text{Link 5: } m_5 = 0.755, \quad \mathbf{r}_{C_5} &= \begin{bmatrix} 0 \\ 0 \\ 0 \end{bmatrix}, \quad \mathbf{I}_5 = \begin{bmatrix} 1.120 & 0 & 0 \\ 0 & 1.227 & 0 \\ 0 & 0 & 0.559 \end{bmatrix} 10^{-3} \\
 \text{Link 6: } m_6 = 0.019, \quad \mathbf{r}_{C_6} &= \begin{bmatrix} 0 \\ 0 \\ -0.007 \end{bmatrix}, \quad \mathbf{I}_6 = \begin{bmatrix} 2.347 & 0 & 0 \\ 0 & 2.347 & 0 \\ 0 & 0 & 4.123 \end{bmatrix} 10^{-6}
 \end{aligned} \tag{18}$$

where the units of mass, length, inertia tensor are kg, m, and kgm^2 , respectively.

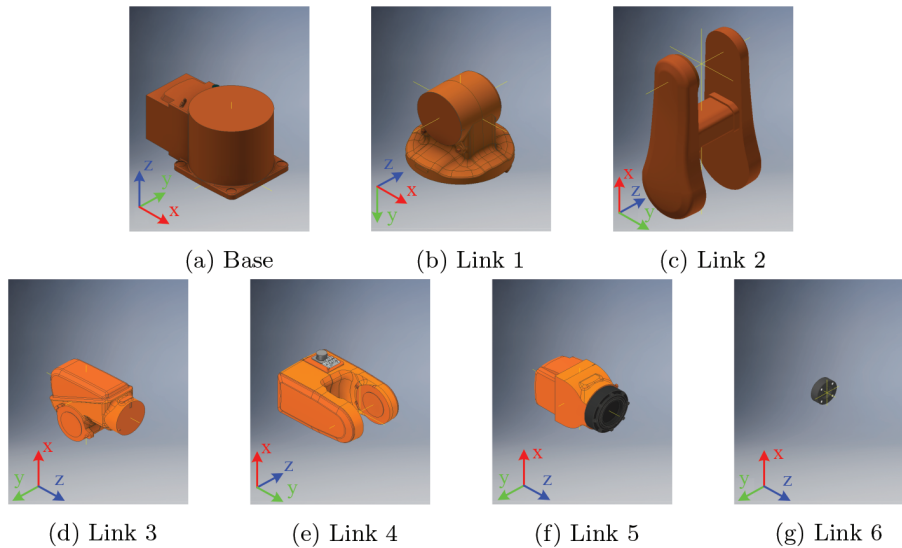


Figure 2. Links of robot IRB 120 designed by Autodesk Inventor.

3.2. Quasi-physical modeling of robot IRB 120

Based on the 3D CAD models containing mass, inertias, joints, and constraints; the quasi-physical modeling of the robot can be built by using Simscape Multibody. For multibody mechanical systems, Simscape Multibody

Under the act of the same input torque, Figure 4b shows that the responses of 2 models are closely matched with slight tracking errors. This result confirms that the quasi-physical model is equivalent to the mathematical model in term of dynamics without friction. Therefore, the quasi-physical model can be used reliably instead of the mathematical model for simulating robot IRB 120.

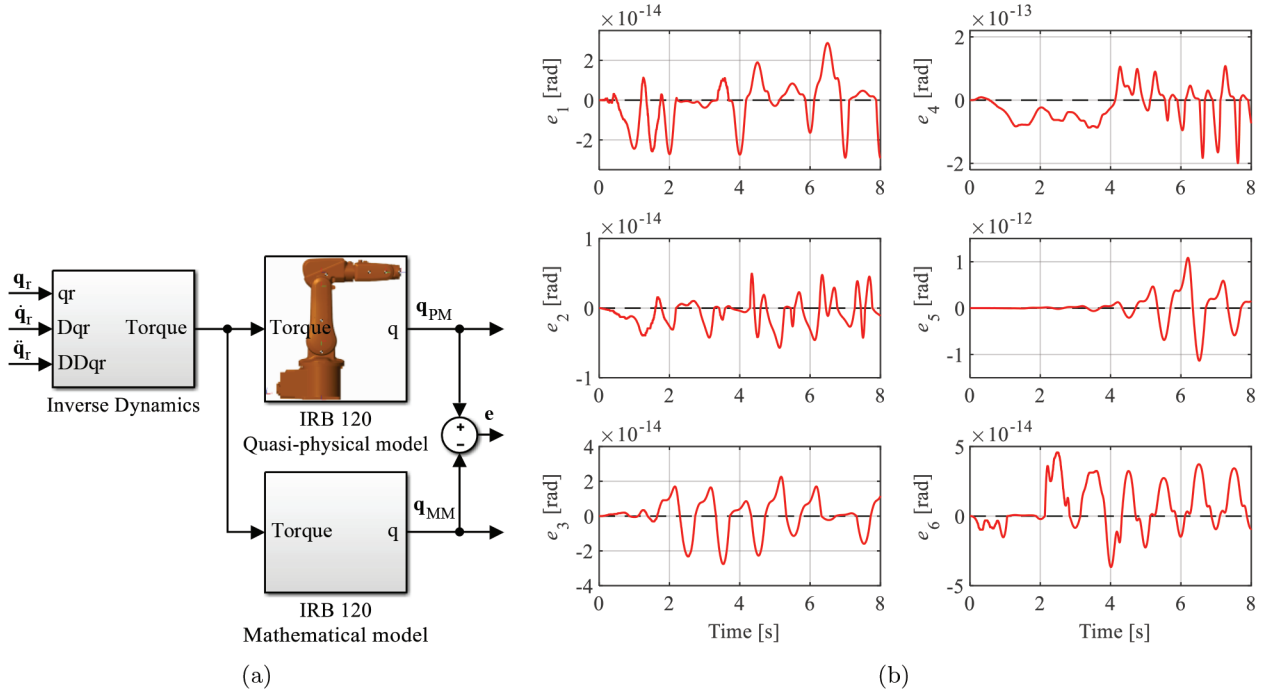


Figure 4. Dynamic simulation diagram for comparison (a) and output errors between 2 models (b).

Next, rotational friction (21) described in Figure 5a can be added to every joint of the quasi-physical model to make the virtual robot closer to the real robot. Friction torque τ_{Fi} which is a function of joint velocity ω_i is approximated in the following equation as the sum of Stribeck τ_{Si} , Coulomb τ_{Ci} , and viscous friction τ_{Vi} [31]:

$$\tau_{Fi} = \sqrt{2}e(\tau_{brki} - \tau_{Ci}) \exp\left(-\left(\frac{\omega_i}{\omega_{Si}}\right)^2\right) \frac{\omega_i}{\omega_{Si}} + \tau_{Ci} \tanh\left(\frac{\omega_i}{\omega_{CLi}}\right) + \tau_{Vi}, \quad (21)$$

where $\tau_{brki} = \tau_{Si(0)} + \tau_{Ci}$ is the breakaway friction torque, $\tau_{Si(0)}$ is the Stribeck friction torque at the vicinity of zero velocity, $\tau_{Vi} = k_{vi}\omega_i$, k_{vi} is the viscous friction coefficient, $\omega_{Si} = \omega_{brki}\sqrt{2}$ and $\omega_{CLi} = \omega_{brki}/10$ are the Stribeck and Coulomb velocity thresholds, ω_{brki} is the breakaway friction velocity at which the Stribeck friction is at its peak: $\tau_{Si(0)}$. The Simscape-based quasi-physical model including all revolute joints with rotational friction (Figure 5b) and their parameters (Figure 5c) for robot IRB 120 is constructed.

The dynamic responses of the mathematical model and the quasi-physical model including joint friction are different despite under the same torque (19) (Figure 6). The Simscape-based simulation indicates that the joints cannot track the references after a few cycles caused by friction effects. This result gives the advantage of using Simscape-based quasi-physical model in the presence of friction.

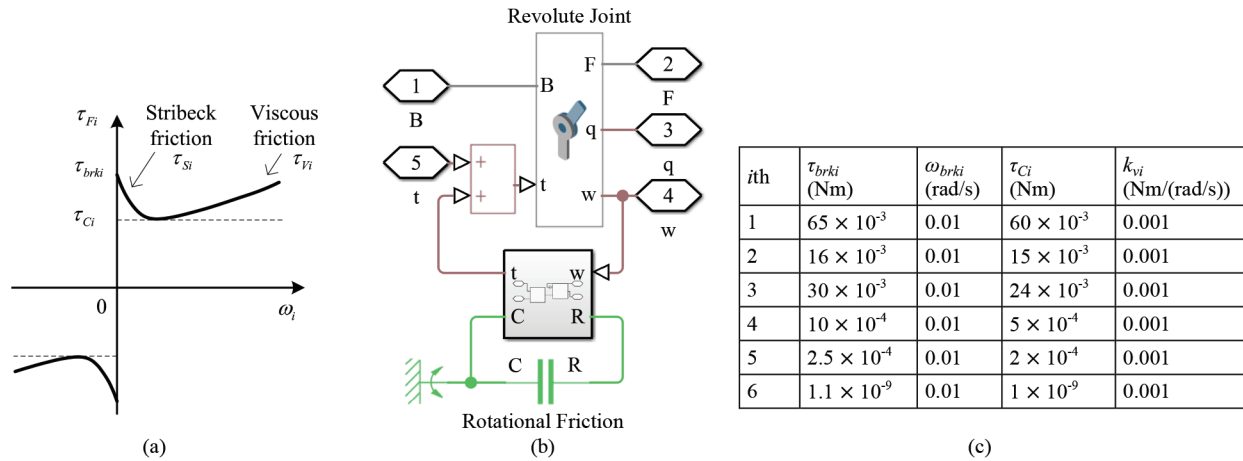


Figure 5. Rotational friction torque (a), Simscape revolute joint with friction (b), and friction parameters (c).

4.2. Control simulation

To illustrate the behaviour of robot IRB 120 under the act of a controller through simulation by using the quasi-physical model, we use a simple control law which depends on the fidelity of parameters of mathematical models is computed-torque control with PD outer-loop as [32]:

$$\tau = \mathbf{M}(\mathbf{q}) (\ddot{\mathbf{q}}_d + \mathbf{K}_d \dot{\mathbf{e}} + \mathbf{K}_p \mathbf{e}) + \mathbf{C}(\mathbf{q}, \dot{\mathbf{q}}) \dot{\mathbf{q}} + \mathbf{g}(\mathbf{q}), \quad (22)$$

where $\mathbf{q}_d = [q_{1d}, q_{6d}]^T$ is the desired trajectory of joints, $\mathbf{e} = \mathbf{q}_d - \mathbf{q}$ is the tracking error; PD parameters $\mathbf{K}_d = \text{diag}(k_{di})$ and $\mathbf{K}_p = \text{diag}(k_{pi})$ are the positive gain diagonal matrices to guarantee the stability of the system. The dynamics of closed-loop error implying asymptotic stability of the system are

$$\ddot{\mathbf{e}} + \mathbf{K}_d \dot{\mathbf{e}} + \mathbf{K}_p \mathbf{e} = \mathbf{0}. \quad (23)$$

For having no overshoot, the PD gains are chosen as $k_{di} = 2\omega_{ni}$ and $k_{pi} = \omega_{ni}^2$ where ω_{ni} is the natural frequency of joint error i . The larger ω_{ni} , the faster response. In the paper, we have selected $[\omega_{n1}, \dots, \omega_{n6}]^T = [15, 15, 15, 25, 25, 30]^T$ for the desired performances at the end of the manipulator faster than near the base.

The control simulation schematic diagrams are shown in Figure 7 for 2 kinds of representing robot IRB 120 by using the quasi-physical model and the mathematical model. The desired trajectories are given as

$$\begin{aligned} q_{1d} &= 2 \sin(2\pi t), & q_{2d} &= 1.5 \sin(2\pi t), & q_{3d} &= \sin(2\pi t) \\ q_{4d} &= 2.5 \sin(2\pi t), & q_{5d} &= 2 \sin(2\pi t), & q_{6d} &= 3 \sin(2\pi t) \end{aligned} \quad (24)$$

Without joint friction and assuming all other parameters are known, Figure 8 shows that the performances of 2 models are similar and all the joints of both models completely follow the desired trajectories after about 0.5 s (Figure 9). The result indicates that the behaviours of the quasi-physical model and the mathematical model are matched if the mathematical model is identified accurately and the quasi-physical model is constructed correctly. In order to express clearly the efficiency of Simscape-based approach, in next simulation, the rotational friction (Figure 5) will be added to the Simscape-based model. The tracking errors depicted in Figure 10 make

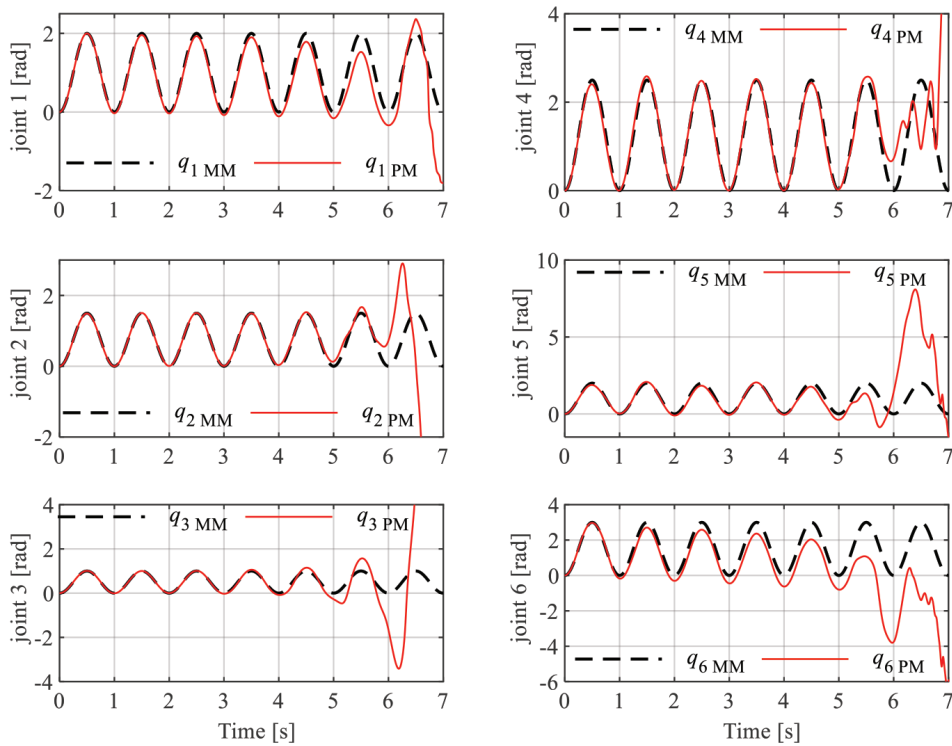


Figure 6. Response comparison between the mathematical model (MM) and the quasi-physical model (PM) including joint friction under the same torque.

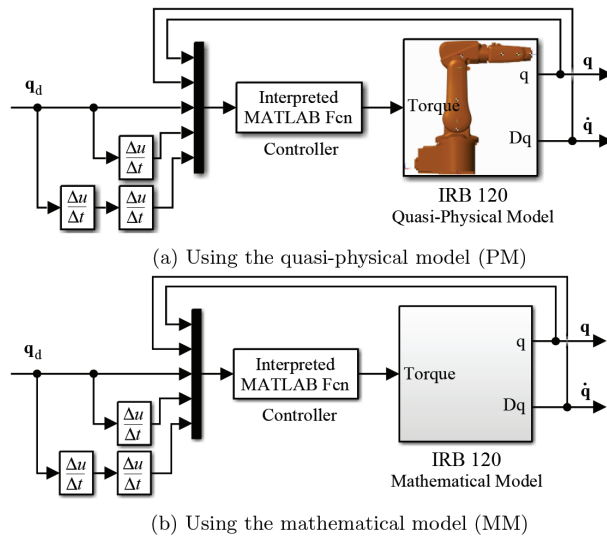


Figure 7. Simulation schematic diagrams with the same control law for robot IRB 120.

the difference between the behaviours of 2 models obviously visible. The joints of the quasi-physical model track the desired trajectories with an oscillation because the feedforward controller (22) cannot compensate perfectly the effects of uncertainty parameters existing in the model.

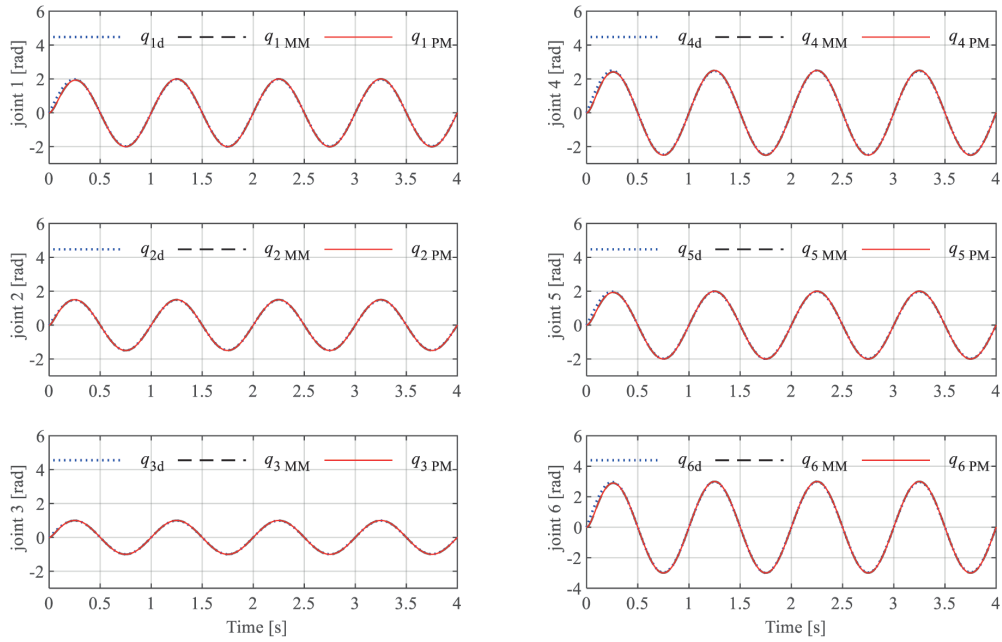


Figure 8. Desired trajectories and responses of the mathematical model (MM) and the quasi-physical model (PM) without friction.

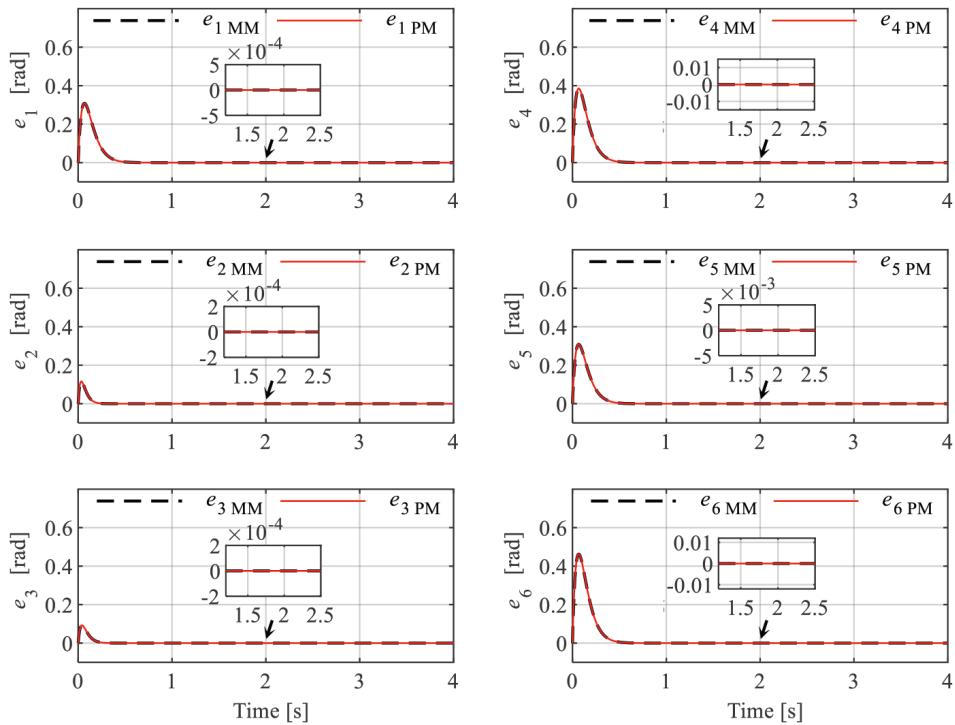


Figure 9. Tracking errors of MM and PM without friction.

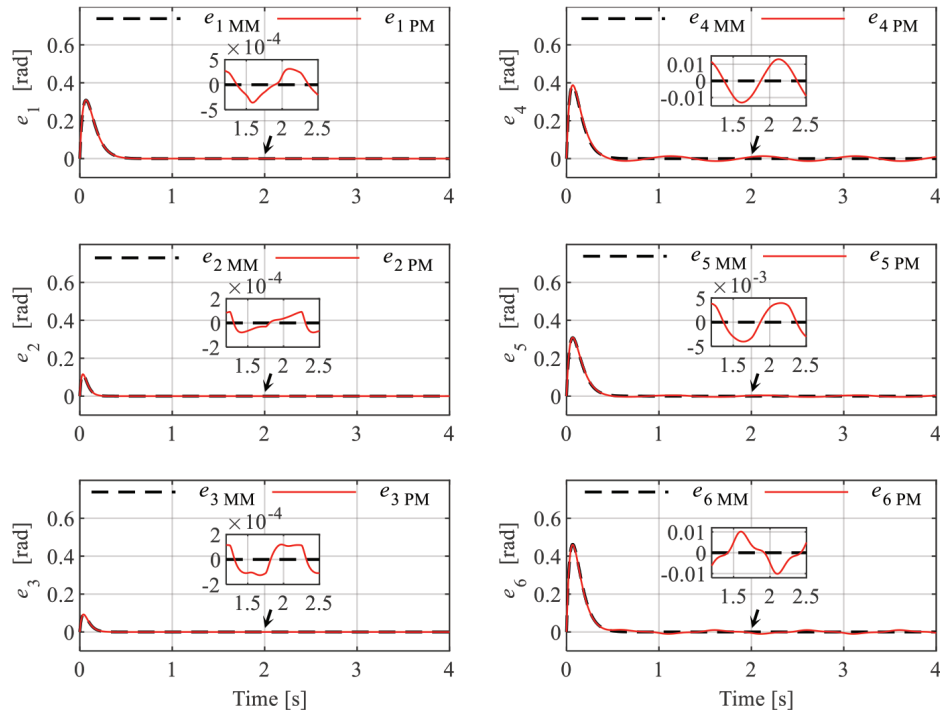


Figure 10. Tracking errors of MM and PM including friction.

5. Conclusions

The dynamic simulation of robot manipulators is conventionally executed with the mathematical model, which is tedious to include complicated terms such as friction and itself cannot guarantee the accuracy of identified parameters and model structure. By using Simscape-based quasi-physical models, the reliability of the dynamic modeling and simulation results are enhanced. Nonlinear components can be added to the model conveniently. The outcomes in this paper show the effectiveness of quasi-physical modeling for robot manipulators using MATLAB/Simscape Multibody. The propriety of a mathematical model can be adjusted and verified by comparing the dynamic response of the model with that of Simscape-based quasi-physical model. Moreover, possible failures in the early design process can be detected by integrating the quasi-physical model with control algorithms before any experiment. This practice-oriented simulation can significantly reduce both time and cost of research and development. In the paper, joint friction is added to compare the effectiveness of Simscape-based modeling and mathematical modeling approaches. In the next investigation, other practical nonlinear issues will be considered.

References

- [1] Angeles J. Fundamentals of Robotic Mechanical Systems: Theory, Methods and Algorithms. 3rd ed. New York, NY, USA: Springer Science+Business Media LLC, 2007.
- [2] Murray RM, Li Z, Sastry SS. A Mathematical Introduction to Robotic Manipulation. Boca Raton, FL, USA: CRC Press, 1994.
- [3] Spong MW, Hutchinson S, Vidyasagar M. Robot Modeling and Control. 1st ed. Hoboken, NJ, USA: John Wiley & Sons, 2006.

- [4] Dombre E, Khalil W (editors). *Modeling, Performance Analysis and Control of Robot Manipulators*. London, UK: ISTE Ltd, 2007.
- [5] Sciavicco L, Siciliano B. *Modelling and Control of Robot Manipulators*. 2nd ed. London, UK: Springer London, 2000.
- [6] Siciliano B, Sciavicco L, Villani L, Oriolo G. *Robotics: Modelling, Planning and Control*. London, UK: Springer London, 2009.
- [7] Basak P, Chowdhury S, Chowdhury SP. Simscape based modeling and simulation of a PV generator in microgrid scenario. In: *22nd International Conference and Exhibition on Electricity Distribution (CIRED)*; Stockholm, Sweden; 2013, pp. 0997 (1-4).
- [8] Joshi S, Mohanty SP, Kougiianos E. Simscape® based ultra-fast design exploration: graphene-nanoelectronic circuit case studies. *Analog Integrated Circuits and Signal Processing* 2016; 87 (3): 407-420.
- [9] Elwarraki E, Mijlad N, Elbacha A. SIMSCAPE electro-thermal modelling of the PIN diode for power circuits simulation. *IET Power Electronics* 2016; 9 (7): 1521-1526.
- [10] Al-Hamadani H, An T, King M, Long H. System dynamic modelling of three different wind turbine gearbox designs under transient loading conditions. *International Journal of Precision Engineering and Manufacturing* 2017; 18 (11): 1659-1668.
- [11] Anatolii S, Naung Y, Oo HL, Khaing ZM, Ye KZ. The comparative analysis of modelling of simscape physical plant system design and armature-controlled system design of DC motor. In: *IEEE Conference of Russian Young Researchers in Electrical and Electronic Engineering (EICoN Rus)*; St. Petersburg, Russia; 2017, pp. 998-1002.
- [12] Waseem M, Suhaib M, Sherwani AF. Modelling and analysis of gradient effect on the dynamic performance of three-wheeled vehicle system using Simscape. *SN Applied Sciences* 2019; 1 (225): 1-13.
- [13] Nunna K, Gautier N, Malack S, Kim M. Model-based design for rapid controller prototyping of Furuta pendulum: A case study using low-cost hardware. In: *UKACC 11th International Conference on Control (CONTROL)*; Belfast, UK; 2016, pp. 1-5.
- [14] Urrea C, Valenzuela L, Kern J. Design, Simulation, and Control of a Hexapod Robot in Simscape Multibody. In: *Valdman J (editor). Applications from Engineering with MATLAB Concepts*. London, UK: InTechOpen, 2016, pp. 126-137.
- [15] Olaya J, Pintor N, Avilés OF, Chaparro J. Analysis of 3 RPS robotic platform motion in simscape and MATLAB GUI environment. *International Journal of Applied Engineering Research* 2017; 12 (8): 1460-1468.
- [16] Nguyen VA, Nguyen AT, Dequidt A, Vermeiren L, Dambrine M. Nonlinear Tracking Control with Reduced Complexity of Serial Robots: A Robust Fuzzy Descriptor Approach. *International Journal of Fuzzy Systems* 2019; 21 (4): 1038-1050.
- [17] Grazioso S, Di Maio M, Di Gironimo G. Conceptual design, control, and simulation of a 5-DoF robotic manipulator for direct additive manufacturing on the internal surface of radome systems. *The International Journal of Advanced Manufacturing Technology* 2019; 101 (5-8): 2027-2036.
- [18] Zátópek J, Uředníček Z, Machado J, Sousa J. Dynamic simulation of the CAD model in SimMechanics with multiple uses. *Turkish Journal of Electrical Engineering & Computer Sciences* 2018; 26 (3): 1278-1290.
- [19] Bingül Z, Karahan O. Dynamic identification of Staubli RX-60 robot using PSO and LS methods. *Expert Systems with Applications* 2011; 38: 4136-4149.
- [20] Schiehlen W, Eberhard P. *Applied Dynamics*. Cham, Zug, Switzerland: Springer International Publishing, 2014.
- [21] Nikravesh PE. *Computer-aided analysis of mechanical systems*. Englewood Cliffs, NJ, USA: Prentice-Hall, 1988.
- [22] Haug EJ. *Computer-Aided Kinematics and Dynamics of Mechanical Systems. Vol. 1: Basic Methods*. Boston, MA, USA: Allyn & Bacon, 1989.
- [23] Shabana AA. *Dynamics of Multibody Systems*. 3rd ed. New York, NY, USA: Cambridge University Press, 2005.
- [24] Shabana AA. *Computational Dynamics*. 3rd ed. Chichester, UK: John Wiley & Sons, 2010.
- [25] Josephs H, Huston R. *Dynamics of Mechanical Systems*. Boca Raton, FL, USA: CRC Press, 2002.

- [26] Khang NV. Consistent definition of partial derivatives of matrix functions in dynamics of mechanical systems. *Mechanism and Machine Theory* 2010; 45 (7): 981-988.
- [27] Khang NV. Kronecker product and a new matrix form of Lagrangian equations with multipliers for constrained multibody systems. *Mechanics Research Communications* 2011; 38 (4): 294-299.
- [28] Brewer J. Kronecker products and matrix calculus in system theory. *IEEE Transactions on Circuits and Systems* 1978; 25 (9): 772-781.
- [29] Laub AJ. *Matrix Analysis for Scientists and Engineers*. Philadelphia, PA, USA: SIAM, 2005.
- [30] Zhang F. *Matrix Theory*. 2nd ed. New York, NY, USA: Springer New York, 2011.
- [31] Armstrong B, de Wit BB. Friction Modeling and Compensation. In: Levine WS (editor). *The Control Handbook*. 1st ed. Boca Raton, FL, USA: CRC Press, 1996, pp. 1369-1382.
- [32] Lewis FL, Dawson DM, Abdallah CT. *Robot Manipulator Control: Theory and Practice*. 2nd ed. New York, NY, USA: Marcel Dekker, 2004.